Neuroradiology (1986) 28: 132-138

Neuroradiology

Spin-echo MR imaging of intracranial hemorrhage

G. C. Dooms,[2] A. Uske[3], M. Brant-Zawadzki[1], W. Kucharczyk[4], L. Lemme-Plaghos[5], T. H. Newton[1], and D. Norman[1]

[1]Department of Radiology, University of California School of Medicine, San Francisco, California, USA
[2]Universite Catholique de Louvain, UCL Saint Luc, Brussels, Belgium
[3]Centre Hospitalier Universitaire Vaudois, Lausanne, Switzerland
[4]Toronto General Hospital, Toronto, Canada, and [5]Instituto de Neurocirurgia, Universidad de Buenos Aires, Argentina

Summary. This retrospective study was performed to describe the appearance of intracranial hemorrhagic lesions on magnetic resonance (MR) imaging at 0.35 tesla using the spin-echo technique, and define the present clinical role of MRI in this particular pathology. Forty-eight examinations of forty-three patients with forty-seven intracranial hemorrhagic lesions (39 true hematomas and 8 hemorrhagic lesions mixed with other tissues) were reviewed for this study. Comparative CT studies were available for all the patients. In our limited experience with acute hematomas (less than 3 days old), low or isointense signal was seen with a short TR (0.5 s), but a relative increase in signal intensity was observed with a long TR (2.0 s). This appearance of acute hematoma was not specific. Chronic hematomas (more than 3 days old) were imaged as foci of bright signal intensity on both short and long TR. This pattern was characteristic of chronic hematoma. With a short TR (0.5 s), two hemorrhagic lesions (5 and 7 days old) were displayed as an isointense signal surrounded by a rim of high intensity signal. This peripheral zone most likely represented liquefaction at the clot's periphery and the initial formation of methemoglobin. T1 and T2 relaxation times were found to be very long for acute hematomas (first two days). T1 values of chronic hematomas (more than 3 days old) were comparatively short and in the same range as T1 of white matter. T2 values of chronic hematomas decreased also but remained very long.

Key words: Intracranial hemorrhage - Magnetic resonance studies - Computed tomographic studies

The capability of MR for the diagnosis of intracranial hemorrhagic lesions has been reported in the literature by several authors [1-5]. More extensive data, [6-8] based on a greater number of patients, described the MR appearance of intracranial hemorrhagic lesions, using the inversion recovery sequence or the spin-echo sequence with only very long TE values. Consequently, the goals of this retrospective study were: a) describe the MR appearance of intracranial hemorrhagic lesions using the spin-echo technique with various combinations of TR and TE parameters and b) define the present clinical role of MRI in this particular pathology.

Materials and methods

Subjects

A retrospective review of 48 MR studies of 43 patients with 47 intracranial hemorrhagic lesions was performed. This group consisted of 23 males and 20 females, ranging in age from 4 days to 76 years. The location and type of the hemorrhagic lesions are described in Table 1. Based on the criteria of one recent published report [8], distinction was made between true hematomas (well defined focal lesions) and homorrhagic tissues (mixture of hemorrhage and other abnormal tissues); the latter were not included in the analysis of T1 and T2 calculations. Some hemorrhagic lesions within brain tumors (3 lesions) were considered true hematomas because of their focal, homogeneous appearance on both the MR study and corresponding CT examination and/or because of surgical proof of a true hematoma within such ab-

Table 1. Location and type of the intracranial hemorrhagic lesions

Location and type	Number of hemorrhagic lesions	Number of patients	Number of MR examinations
True hematomas	39	35	39
intraaxial	31	29	32
extraaxial	8	6	7
subdural hematoma	5	3	4
subarachnoid hemorrhage	3	3	3
Hemorrhage mixed with other tissues	8	8	9
hemorrhage in brain tumors	7	7	7
hemorrhagic infarcts	1	1	2
Total number	47	43	48

normal tissues. Thus, 39 true hematomas were used in the final analysis of relaxation values.

The etiologies of the 39 true hematomas were arteriovenous malformations (23 lesions), trauma (7 lesions), brain tumors (3 lesions), hypertension (1 lesion), thrombocytopenia (2 lesions) and unknown origin (3 lesions). Seven hemorrhages within brain tumors and one hemorrhagic infarct were also reviewed.

These hemorrhagic lesions were confirmed by surgery (24 lesions), lumbar puncture (3 lesions) or computed tomography together with definitive clinical history (20 lesions). The ages of the hemorrhagic lesions were determined from the clinical history of the patients, and were divided into acute (less than 3 days old) and subacute and chronic hematomas (more than 3 days old). By these criteria, four hematomas were acute, while thirty-five were subacute or chronic.

Computed tomographic studies were available for comparison in all patients: both studies were always performed within a seven-day period.

Technical considerations

Proton MR imaging was performed using a 0.5 tesla superconducting magnet operating at 0.35 tesla (proton resonance frequency of 15 MHz) and a head coil 25 cm in diameter (Diasonics MT/S). The features of this imager have been previously described [9]. At the time the study was done, images were reconstructed on a 128 by 128 display matrix. Section thickness was 7 mm with a 3 mm gap between sections.

A multislice, double spin-echo imaging technique was utilized in all cases, with echo delay times (TE) of 28 and 56 ms and pulse sequence repetition times (TR) of 0.5 and 2.0 sec. The 0.5/28 technique provided images with contrast based on significant T1 differences, while the 2.0/56 technique provided images predominantly based on T2 contrast.

The CT examinations were performed with a GE 8800 CT/T or GE 9800 CT/T scanner. Intravenous contrast material was used in one-half of the cases. The slice thickness was 10 mm.

Image analysis

Signal intensity in absolute numbers (mean intensity values) was obtained by circumscribing a region of interest (ROI) with a cursor on the displayed image. The ROI was always greater than 15 pixels to obtain more reliable values. Measurements of MR signal intensity for the different regions of interest, hemorrhagic foci and normal white matter) were recorded.

The absolute intensity of a particular tissue with one particular imaging sequence has little significance. Therefore, determination of the absolute signal intensity was performed not only for the hemorrhagic lesions but also for the normal white matter (reference tissue). The percent of contrast of hemorrhagic lesion versus white matter was calculated as follows:

$$\%\ \text{contrast} = \frac{\text{intensity of hemorrhagic lesion} - \text{intensity of white matter}}{\text{intensity of hemorrhagic lesion} + \text{intensity of white matter}} \times 100$$

The estimation of T1 and T2 values was calculated by the computer based on the previously described formula [9]. The T1 values obtained at different TR combinations were standardized by using a correction factor [10]. The T1 and T2 relaxation times were determined for white matter, as well as for the hemorrhagic lesions.

The MR and CT studies were analyzed with both scans available and in conference by at least two experienced observers. The specific components of interest were the intensity changes with various imaging parameters, the appearance of the hemorrhagic lesion and of the surrounding tissues.

Statistical analysis

All the data were expressed as group mean ± one standard deviation. Comparisons between the multiple different groups were made by analysis of variance. When a statistical significance was found be-

Table 2. Relaxation times of various brain tissues

Type of tissue	T1 relaxation time (ms) (mean ± SD)	T2 relaxation time (ms) (mean ± SD)
normal white matter	419 ± 28	53 ± 3
acute hematomas (< 3 days)	839 ± 158	81 ± 2
chronic hematomas (> 3 days–4 months)[a]	427 ± 51	70 ± 8

[a] The T1 and T2 relaxation times of chronic hematomas remained constant with time

Table 3. Percent contrast hemorrhagic lesion versus normal white matter (%)

	Acute hematoma versus white matter (4 lesions)	Subacute or chronic hematoma versus white matter (31 lesions)
TR = 0.5 s TE = 28 ms	0 ± 5	17 ± 6
TR = 0.5 s TE = 56 ms	8 ± 4	23 ± 7
TR = 2.0 s TE = 28 ms	20 ± 2	15 ± 6
TR = 2.0 s TE = 56 ms	30 ± 3	21 ± 6

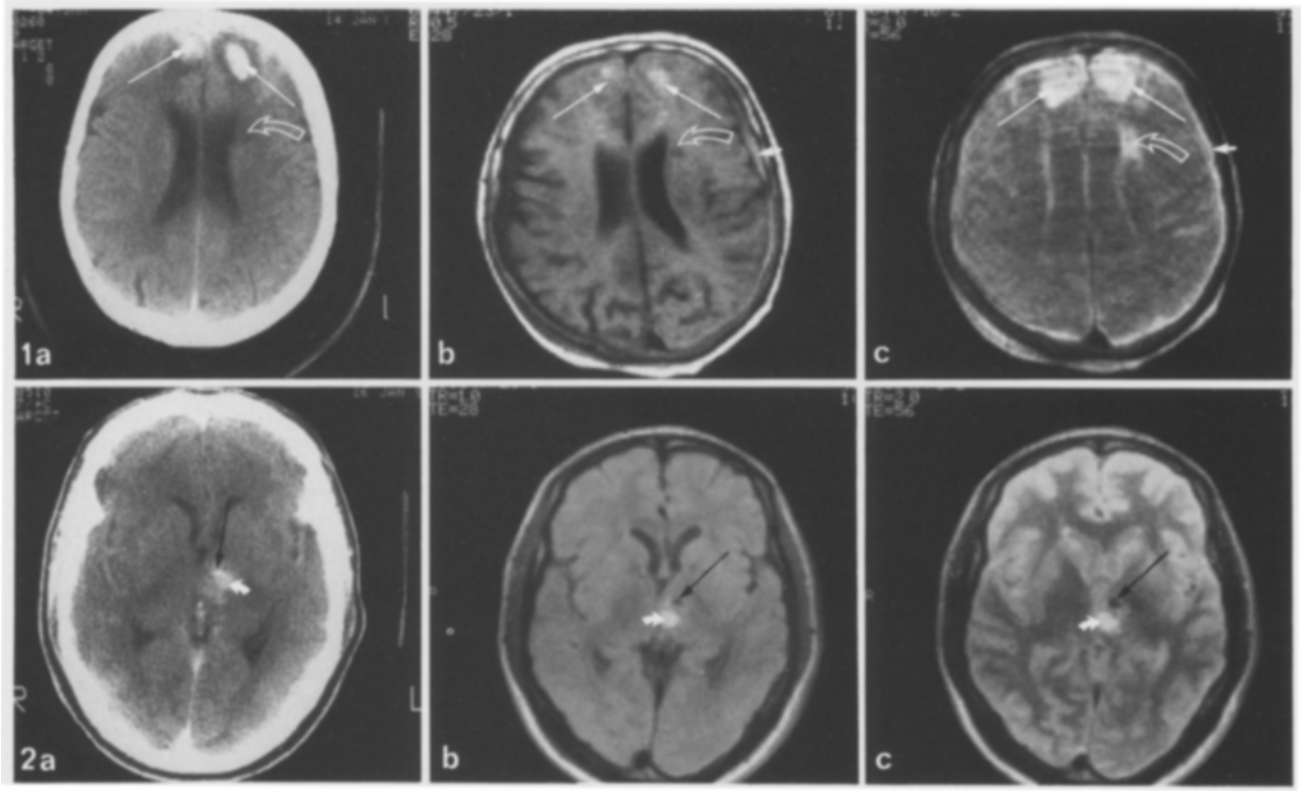

Fig. 1 a–c. Demonstration of acute bifrontal hematomas, left subdural hematoma nine hours after head trauma, and an old infarct in the left caudate nucleus (*long arrow* = acute frontal hematoma, short arrow = acute subdural hematoma, *open curved arrow* = infarct in the left caudate nucleus). **a** Precontrast CT image demonstrates the acute bifrontal hematomas as homogeneous hyperdense lesions, surrounded by a low density rim. The left subdural hematoma was identified by using a modified window. Slightly hypodense lesion in the left caudate nucleus (old infarct). **b, c.** MR images at the same level as (**a**), done 2 h later (11 h). Two different combinations of TR and TE parameters (B: TR = 0.5 s and TE = 28 ms; C: TR = 2.0 s and TE = 56 ms). Acute bifrontal hematomas and left subdural hematoma appear minimally hyperintense compared to white matter, while the caudate infarct appears hypointense on (**b**); all are imaged with higher signal intensity than normal brain on (**c**). No peripheral zone (edema) could be distinguished from the acute hematomas on MRI. Notice the image degradation due to patient motion

Fig. 2 a–c. Demonstration of subacute hematoma (5 days old) secondary to cryptic arteriovenous malformation in the left thalamus (*black arrow* = calcification, *curved arrowhead* = subacute hematoma). **a** Contrast enhanced CT image demonstrates an anterior hyperdense focus in the left thalamus suggesting calcification. The rest of the lesion is imaged as an area of fainter hyperattenuation and it is not possible to determine whether this is due to hemorrhage or calcium. **b, c** MR images at the same level as (**a**). Two different combinations of TR and TE parameters (**b**): TR = 1.5 s and TE = 28 ms; **c**: TR = 2.0 s and TE = 56 ms). On (**b**) and (**c**), the anterior signal dropoff is typical of calcification and corresponds to the high density area seen on CT. On (**b**) and (**c**), the posterior part of the lesion is imaged with high intensity. This is typical of subacute hematoma

tween these multiple groups (i.e., when P values were < 0.05), a statistical test of Newman-Keuls was performed to identify the pairs of groups.

Results

Acute hematomas (less than 3 days old)

The T1 and T2 relaxation values of acute hematomas were very long and longer than those of white matter (Table 2). When compared to white matter, such acute bleeding (less than 3 days old) was imaged as a relatively isointense lesion on the short TR (0.5 s) and short TE (28 ms)-percent contrast versus white matter = 5% (Fig. 1 b). It showed an increase in intensity with a longer TE of 56 ms. A more obvious increase in intensity was seen with a longer TR of 2.0 s. A longer TE (56 ms) further added to the contrast of blood on the longer TR sequences (Table 3) (Fig. 1 c). Therefore, when a long TR of 2.0 s and either a short or long TE were used, the intensity signal of the fresh blood was significantly greater than that of white matter ($P < 0.001$ for both).

With CT, acute hemorrhagic lesions were easily identified as such when relatively homogeneous masses having high CT density numbers was seen; the lesions were surrounded by a peripheral zone of low density, presumably edema (Fig. 1 a). With MR, these acute lesions were also displayed as relatively homogeneous masses with the different TR/TE pairs (Fig. 1 b) and 1 c). However, no peripheral zone

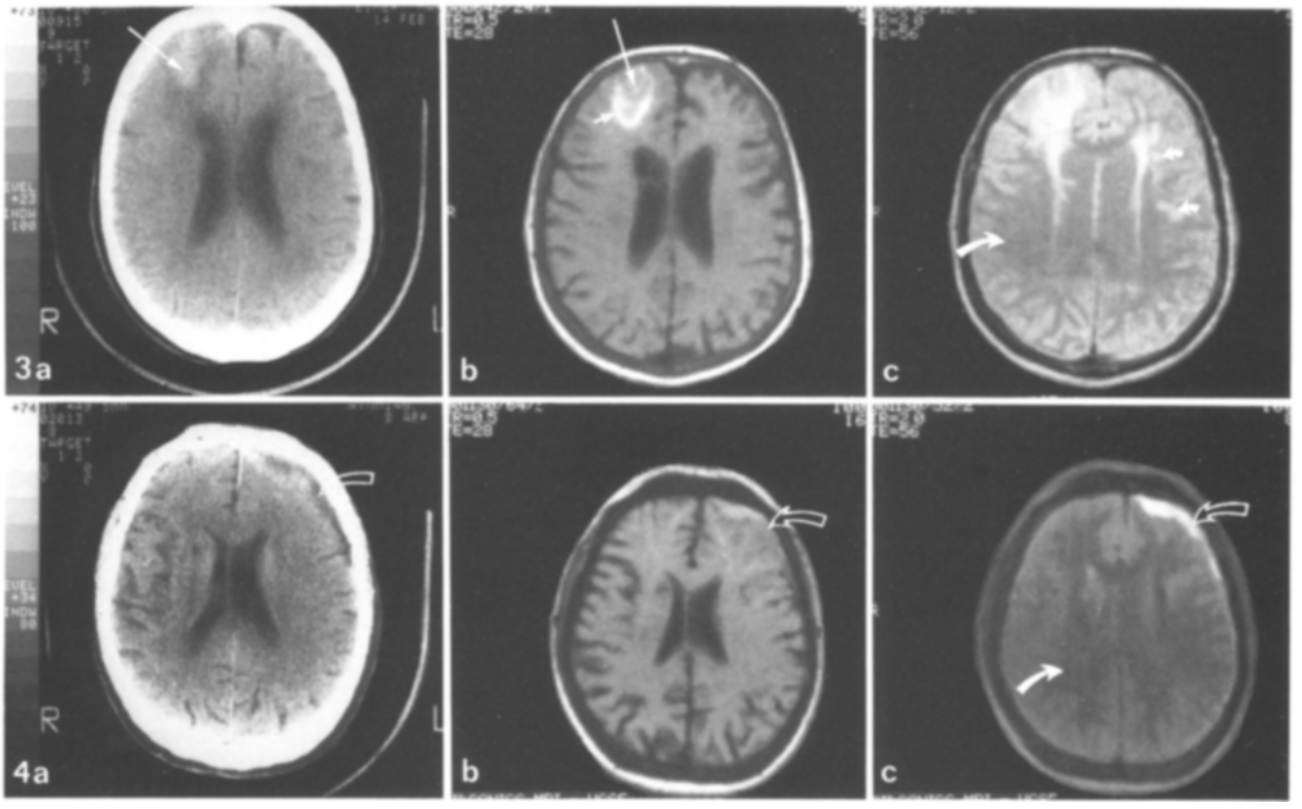

Fig. 3a–c. Demonstration of a two component hematoma (7 days old) in the right frontal lobe due to trauma (*long arrow* = clot, *short arrow* = serum, *curved arrow* = white matter) **a** Precontrast CT image demonstrates a slightly hyperdense and homogeneous lesion in the right frontal lobe (clot), surrounded by a rim of low density (serum and surrounding edematous reaction). **b, c** MR images at the same level as (**a**). Two different combinations of TR and TE parameters (**b**: TR = 0.5 s and TE = 28 ms; **c**: TR = 2.0 s and TE = 56 ms). On (**b**), the lesion displayed a high intensity rim (serum) around an isointense center (clot) relative to white matter. On (**c**), the lesion appears greater in size and is imaged as a high intensity lesion. The different components (clot, serum and surrounding edematous reaction) are indistinguishable on (**c**). On (**c**), multiple small infarcts are depicted with high signal intensity in the left deep white matter *(curved arrowheads)*

Fig. 4a–c. Demonstration of left chronic subdural hematoma in a patient with progressive hemiparesis (*open curved arrow* = chronic subdural hematoma, *curved arrow* = white matter). **a** Precontrast CT image demonstrates left hypodense subdural collection (hematoma). The age of the bleeding was impossible to determine from the clinical history. **b, c** MR images at the same level as (**a**). Two different combinations of TR and TE parameters (**b**: TR = 0.5 s and TE = 28 ms; **c**: TR = 2.0 s and TE = 56 ms). The chronic subdural hematoma appears isointense with normal white matter on (**b**) and is imaged with higher signal intensity than normal white matter on (**c**). It follows the same trends as an acute hematoma

could be distinguished from the acute hematoma suggesting the inability to separate acute hemorrhage from edema. One patient with bifrontal, acute hematomas also harbored a small old infarct in the left caudate nucleus. Although these lesions were readily identified with MR, they presented similar intensity changes as the infarct on the long TR sequence (Fig. 1c).

Subacute or chronic hematomas (more than 3 days old)

The percent contrast, chronic hematoma versus normal white matter is presented in Table 3. Thirty-five subacute or chronic hematomas (33 patients and 37 MR examinations) were reviewed. No distinction could reliably be made by MR criteria between subacute (3–14 days) and chronic hematomas in our material.

In 31 hemorrhagic lesions (30 patients and 34 MR examinations), subacute or chronic hematoma (more than 3 days old) yielded a bright intensity with a short TR of 0.5 s and a short TE of 28 ms (percent contrast versus white matter = $17 \pm 6\%$) (Fig. 2b). The percent contrast between chronic hematoma and white matter was approximately the same with a longer TR and increased slightly with a longer TE (Table 3) (Fig. 2c). With the various different TR/TE pairs, chronic hematoma was of significantly higher intensity than white matter ($P < 0.001$ for the four pairs). A long TR of 2.0 s and either a short or long TE did not permit the distinction of chronic hematoma from acute hematoma ($P < 0.2$ and < 0.1, respectively). The use of a short TR of 0.5 s and ei-

ther a short or long TE did so reliably ($P < 0.005$ and < 0.025, respectively).

T1 values of chronic hematomas were shorter than those of acute hematomas and in the same range as T1 of white matter (Table 2). T2 values of chronic hematomas were shorter than those of acute hematomas but remained long relative to white matter (Table 2). The T1 and T2 relaxation values of chronic hematomas remained constant with aging, the oldest sampled bleed in this series being four months.

With CT, the 31 hemorrhagic lesions were displayed as slightly hyperdense in one-half of the lesions (Fig. 3a) and iso- or hypodense in the other half. In the latter instances, the presence of hemorrhagic component to the lesion was often very difficult to demonstrate with CT and was only possible retrospectively by comparison with prior CT studies or with the corresponding MR examination. MR displayed the chronic hematomas as relatively homogeneous masses of very bright signal intensity with the different TR/TE pairs (Fig. 3b and c).

One morphologic pattern was associated with two subacute hematomas; two hemorrhagic lesions (one posttraumatic hematoma in the right frontal lobe and one true hematoma within an acoustic neurinoma - 5 and 7 days old, respectively) displayed a distinct MR pattern. On the short TR of 0.5 s and either a short or long TE, they displayed a relatively bright rim of signal around an isointense center relative to white matter (Fig. 3b). With a longer TR of 2.0 s and either a short or long TE, both the central part of the hemorrhagic lesion and the rim were imaged as a bright intensity signal and were indistinguishable (Fig. 3c). Furthermore, the lesion appeared greater in size with a long TR than with a short TR (Fig. 3b and c). The evolutionary intensity pattern of the rim surrounding the lesion, with various imaging parameters, was the same as that of other subacute and all chronic hematomas.

With CT, the hemorrhagic lesion appeared as an hyperdense and homogeneous lesion, surrounded by a rim of low density (Fig. 3a). When comparing the two examinations, the hyperdense lesion displayed with CT corresponded in size to the central part and rim seen with MR (Fig. 3). With a long TR of 2.0 s, the enlarged lesion of very bright signal intensity displayed with MR corresponded to both the hyperdense area plus the rim of low density seen with CT (Fig. 3).

Bilateral subdural hematomas in one patient were imaged as slightly hypodense with CT examination (Fig. 4a). Surprisingly, with a short TR of 0.5 s, unlike the other chronic hematomas, they appeared as a relatively isointense signal when compared to white matter (Fig. 4b). These bilateral subdural hematomas followed the same trends as acute bleeding (Fig. 4b and c). Unfortunately, the age of the bleeding was impossible to determine from the clinical history of this patient, an elderly male with progressive hemiparesis.

Hemorrhages mixed with other lesions

On hemorrhagic infarct was imaged twice with MR (three and nine weeks old). Its MR appearance and evolutionary features have been described previously [3].

Six hemorrhages in various brain tumors were also reviewed. The hemorrhagic site within the tumor was always imaged as a bright signal intensity compared to surrounding tumoral tissue with a short TR of 0.5 s. The hemorrhagic site and surrounding tumoral tissue were almost indistinguishable when a long TR of 2.0 s was used.

Discussion

On spin-echo images, signal intensity is relatively high in tissues with short T1, long T2 and high spin density. The relative contribution of T1 and T2 depends on the TR and TE values of the chosen pulse sequence, as well as the field strength of the imager. T1 differences are accentuated on images obtained with a short TR (0.5 s at our field strength). T2 differences are best evaluated on images obtained with a long TE of 56 ms or more. As fresh blood has long T1 relaxation time, its signal intensity is intermediate on images obtained with a short TR of 0.5 s and a short TE of 28 ms. However, chronic hematoma has a relatively short T1 and therefore is imaged with a bright signal intensity on images performed with the same parameters. The shortening of T1 relaxation time of subacute or chronic hematoma compared to acute hematoma could be explained by the oxidation of hemoglobin to the methemoglobin form, a paramagnetic substance that affects T1 [11, 12]. This occurs at approximately 3-4 days, and may explain the high intensity ring in some of our subacute hematomas, in which the center still has the characteristics of an acute hemorrhage. As both acute and chronic hematomas have long T2 relaxation times, when compared to white matter, their relative intensity increased with a long TE of 56 ms. The shorter T2 of chronic as compared to acute hematomas may also be an effect of methemoglobin (or other paramagnetic species) formation.

The double spin-echo technique performed with both a short and a long TR is well suited to investigate the chronic hemorrhagic lesions. A short TR of 0.5 s and short TE of 28 ms is helpful to depict the

relatively specific bright signal intensity of the chronic hematoma and of the hemorrhagic sites in brain tumors and to differentiate the central zone from the rim in some subacute hemorrhagic lesions. A long TR of 2.0 s is also useful because the best contrast between acute bleeding and white matter is obtained with a long TR of 2.0 s and a long TE of 56 ms. Unfortunately, the acute hemorrhages were difficult to characterize as such, appearing like other lesions with long T1 and T2 on the spin-echo sequences. Patients with acute intracranial hemorrhage are difficult to study with MRI, as they are often uncooperative or on life support equipment, thus our experience is limited. An acute hematoma may show hypointensity or isoitensity on short TR sequences, depending on the balance of long T1 or long T2 components achieved in affecting signal intensity (28 ms, minimum, of T2 effect is present in our sequences).

With computed tomography (CT), hematomas have characteristic evolutionary features for their density. Nearly 100% of the subdural hematomas are hyperdense in the first week [13], exceptions being those in severely anemic patients. The relative hyperdensity of recent hemorrhage compared with surrounding normal brain on precontrast scans is an obvious finding that permits a specific diagnosis in most of the cases [14–16]. With time, clot resorption leads to diminution of CT density and occurs at a variable rate [16–18]. By day 22, 10% of subdural hematomas remain hyperdense [13]. In the acute phase, CT demonstrates the region surrounding hematomas as an irregular decreased density consistent with edema [19–21]. This rim becomes slightly wider during the first week, representing in part a density reduction in the outer margins of the hematoma itself, as well as edematous changes in the surrounding brain [21]. Low attenuation around dense clot represents expressed serum or fluid from clot resorption induced by granulation tissue that begins at the periphery and extends centrally [14–16].

With MR imaging, the intensity of the hemorrhagic lesions varies also characteristically but not in the same way as CT. In the acute phase, with all the different TR/TE pairs, MR cannot distinguish between the hematoma itself and the edematous surrounding tissue because of similar long T1 and T2 relaxation times of edema [22]. After 3 days, the hematoma is imaged with a relatively characteristic bright signal intensity on the short TR of 0.5 s (short T1) and therefore, allows a clear distinction from contusion and edema that appear as dark or isointense with this TR (long T1) [23]. With a long TR and TE, this distinction cannot be made because of similar long T2 relaxation times of hematoma, contusion and edema. The MR appearance of hemorrhagic lesions as a central zone of isodense signal surrounded by a rim of bright signal intensity has been described previously [1, 2, 6, 7]. In view of the knowledge of the CT evolution of the hematomas (see above), the central zone most likely corresponds to the dense portion of the acute hematoma or clot seen with CT. The low density rim displayed with CT is divided in two dinstinct parts by MRI when a short TR is used: a bright signal intensity rim corresponding to expressed serum from clot resorption (within which the paramagnetic effects of methemoglobin may well be in effect) and a surrounding isodense signal (compared to white matter) corresponding to edematous changes in the brain surrounding the hematoma. When a long TR and TE are used, these three different components are summed together as bright signal intensity lesions and cannot be distinguished (due to their similar long T2 relaxation times) at our field strength. The MR signal intensity of the hematomas older than 3 days remain the same as a result of nonsignificant changes of the intrinsic relaxation parameters with aging.

The hemorrhagic sites in brain tumors were displayed as bright signal intensity on the short TR of 0.5 s. Surgery proved that all these lesions represented in fact old hemorrhages. It is presumed that acute hemorrhage within brain tumors cannot be distinguished from the brain tumor because of the similarity of the intrinsic relaxation parameters (long T1 and T2 relaxation times) and of the similar intensity patterns with various imaging parameters.

One report [2] mentioned one brain hemorrhagic lesion followed for 7 months after the original scan, where the MR examination shows a residual long T1 area. The same pattern was encountered in one patient with bilateral subdural hematomas. The long-term evolution of the intrinsic relaxation parameters of a hematoma (more than 6 months or one year) are unknown at this time.

The present clinical role of MRI for the demonstration of brain hemorrhagic lesions depends on the stage of the lesion. In the acute phase (first two days), the role of MR is limited. MR is often very difficult to perform in patients with mechanical life support equipment or significantly depressed mental states (Fig. 1b and c). Furthermore, the CT appearance of acute hemorrhagic lesions is nearly pathognomonic [14–16]. The nonspecific MR features for acute hematomas are similar to many other disease processes (infarcts, tumors, edema . . .) both being characterized by long T1 and T2 relaxation times.

In the subacute and chronic phase (after 3 days), MRI can play a very important role in the demonstration and characterization of hematomas. The CT demonstration of subacute and chronic hemorrhagic lesions is more difficult than in the acute phase and can sometimes be based only on the recognition of

indirect signs [24, 25]. The characteristic bright signal intensity of the subacute and chronic hematomas on a short TR of 0.5 s is very helpful in the demonstration of these lesions. Furthermore, no other lesion mimics the signal intensity pattern of the subacute and chronic hematomas, except the rare benign brain lipomas. They can be imaged with the same intensity patterns as those of subacute and chronic hematomas on all the different TR/TE pairs [26]. However, the T1 and T2 relaxation times of benign lipomas are usually shorter than those of subacute and chronic hematomas [26]. Another method to differentiate lipomas from subacute and chronic hematomas is the use of chemical shift imaging [27]. Finally, it should be mentioned that the experience reported herein is in the context of 0.35 T, and that some of the concepts expressed may well vary at a much higher field strength.

Conclusion

The bright signal intensity of subacute and chronic hematomas (more than 3 days old) on a short TR of 0.5 s is relatively pathognomonic and is very helpful in the demonstration and characterization of chronic hematomas. At this time, the role of MRI is relatively limited in the acute phase given the limitations of the technique and the nearly pathognomonic hyperdense appearance of the acute hematomas on the more easily performed precontrast CT examination.

References

1. Bailes DR, Young IR, Thomas DJ, et al. (1982) NMR imaging of the brain using spin-echo sequences. Clin Radiol 33: 395-414
2. Bydder GM, Steiner RE, Young IR, et al. (1982) Clinical NMR imaging of the brain: 140 cases. AJNR 3: 459-480
3. Crooks LE, Ortendahl DA, Kaufman L, et al. (1983) Clinical efficiency of nuclear magnetic resonance imaging. Radiology 146: 123-128
4. Sipponen JT, Sepponen RE, Sivula A (1984) Chronic subdural hematoma: Demonstration by magnetic resonance. Radiology 150: 79-85
5. Moon KL Jr, Brant-Zawadzki M, Pitts LH, et al. (1984) Nuclear magnetic resonance imaging of CT-isodense subdural hematomas. AJNR 5: 319-322
6. Sipponen JT, Sepponen RE, Sivula A (1983) Nuclear magnetic resonance (NMR) imaging of intracerebral hemorrhage in the acute and resolving phases. JCAT 7: 954-959
7. Han JS, Kaufman B, Alfidi RJ, et al. (1984) Head trauma evaluated by magnetic resonance and computed tomography: A comparison. Radiology 150: 71-77
8. Da La Paz RL, New PFJ, Buonanno FS, et al. (1984) NMR imaging of intracranial hemorrhage. JCAT 8: 599-607
9. Crooks L, Arakawa M, Hoenninger J, et al. (1982) Nuclear magnetic resonance whole-body imager operating at 3.5 KGauss. Radiology 143: 169-174
10. Ehman RL, Kjos BO, Brasch RC, et al. (1984) Spin-echo imaging: Method for correction of systematic errors in calculated T1 and spin density. Presented at the Third Annual Meeting of the Society of Magnetic Resonance in Medicine. New York, August 13-17
11. Koenig SH, Brown RD III, Lindstrom RT (1981) Interactions of solvent with the heme region of methemoglobin and fluoromethemoglobin. Biophys J 34: 397-408
12. Bradley WA, Schmidt PG (1984) The changing MRI appearance of subarachnoid hemorrhage: Effect of methemoglobin formation. Presented at the Third Annual Meeting of the Society of Magnetic Resonance in Medicine. New York, August 13-17
13. Scotti G, Terbrugge K, Melancon D et al (1977) Evaluation of the age of subdural hematomas by computerized tomography. J Neurosurg 47: 311-315
14. Wolverton MK, Creeps LF, Sundaram M, et al. (1983) Hyperdensity of recent hemorrhage at body computed tomography: Incidence and morphologic variation. Radiology 148: 779-784
15. Butzer JF, Cancilla PA, Cornell SH (1976) Computerized axial tomography of intracerebral hematoma. A clinical and neuropathological study. Arch Neurol 33: 206-214
16. Dolinskas CA, Bilaniuk LT, Zimmerman RA, et al. (1977) Computed tomography of intracerebral hematomas. I. Transmission CT observations on hematoma resolution. AJR 129: 681-688
17. New PFJ, Aronow S (1976) Attenuation measurements of whole blood and blood fractions in computed tomography. Radiology 121: 635-640
18. Messina AV, Chernik NL (1975) Computed tomography: The "resolving" intracerebral hemorrhage. Radiology 118: 609-613
19. Muller HR, Wuthrigh R, Wiggli U, et al. (1975) The contribution of computerized axial tomography to the diagnosis of cerebellar and pontine hematomas. Stroke 6: 467-475
20. Scott WR, New PFJ, Davis KR, et al. (1974) Computerized axial tomography of intracerebral and intraventricular hemorrhage. Radiology 112: 73-80
21. Dolinskas CA, Bilaniuk LT, Zimmerman RA, et al. (1977) Computed tomography of intracerebral hematomas. II. Radionuclide and transmission CT studies of the perihematoma region. AJR 129: 689-692
22. Brant-Zawadzki M, Bartkowski HM, Pitts LH, et al. (1984) NMR imaging of experimental and clinical cerebral edema. Noninvasive Med Imag 1: 43-47
23. Young IR, Bydder GM, Hall AS, et al. (1983) Extracerebral collections: Recognition by NMR imaging. AJNR 4: 833-834
24. Moller A, Ericson K (1979) Computed tomography of isoattenuating subdural hematomas. Radiology 130: 149-152
25. Amendola M, Ostrum BJ (1977) Diagnosis of isodense subdural hematomas by computed tomography. AJR 129: 693-697
26. Dooms GC, Hricak H, Sollitto RA, et al. (1985) MR of lipomatous tumors and tumors with fatty component: Comparison with CT
27. Rosen BR, Carter EA, Pykett IL, et al. (1985) Proton chemical shift imaging: An evaluation of its clinical potential using an *in vivo* fatty liver model. Radiology 154: 469-472

Received: 7 May 1985

Dr. M. Brant-Zawadzki
Department of Radiology
University of California School of Medicine
San Francisco, CA 94143
USA